JOURNAL OF AIRCRAFT
Vol. 33, No. 5, September–October 1996

Wing in Heaving Oscillatory Motion

Reza Karkehabadi* and Dean T. Mook†
Virginia Polytechnic Institute and State University, Blacksburg, Virginia 24061-0219

A wing in steady flight near a wavy surface, such as in the case of a large, transoceanic wingship, is simulated by a wing oscillating in heave near a flat surface. In accord with the wingship, small AR and slight camber are considered. In the present study, consideration is limited to the case when the wavelength of the surface is much greater than the chord of the wing and the slope of the surface is much less than unity. The numerical simulation predicts that the mean aerodynamic loads on a wing executing a simple-harmonic heaving motion are higher than the corresponding loads on the same wing in steady flight at the mean height and the same angle of attack. These preliminary results suggest that it would be beneficial to fly near the waves and that doing so would improve the aerodynamic efficiency. Also included in the present results are numerical simulations of the wakes that show the strong influences of the ground and the oscillations on their behavior.

I. Introduction

BECAUSE there is a marked increase in the ratio of lift-to-drag that occurs when a wing flies near the ground, there is an interest in designing airplanes to operate near the ground: one example is the wingship proposed by Aerocon, Inc.[1] and others are the so-called ekranoplans (some as large as a DC-9) designed, built, and flown in the former Soviet Union. An airplane can fly near the surface of the ocean from continent to continent; hence, one application of such craft is transoceanic flight. One of the fundamental questions that has not received much attention to date is how will the ocean waves effect the performance. In this article we address this question.

The vortex–lattice method has been widely used for steady and unsteady aerodynamics for thin and thick, lifting, and non-lifting bodies. Belotserkovskii[2] obtained the steady normal force and moment about the leading edge for a unit-AR rectangular flat plate taking into account wingtip separation. The method was applied to a delta wing by Mook and Maddox.[3] Konstadinopoulos et al.[4] further extended the method and presented results for the same configurations.

Steven[5] studied the landing performance of an aircraft. The flow during takeoff and landing is unsteady even if the aircraft is moving with constant velocity. The phenomenon of ground effect is also observed in ship motion near a canal wall or near a second ship. Exact solutions for three-dimensional wings are most likely impossible to obtain.[6] Since experimental work is a difficult and expensive task for wings in ground effect,[7] a numerical technique is valuable. Nuhait and Mook[8] used the vortex–lattice method to calculate the aerodynamic load in and out of ground effect. They used the method of images to enforce the no-penetration condition at the ground. Their results compare with the experimental data of Chang.[9] Chen and Schweikhard[10] solved for the unsteady ground effect for a two-dimensional flat plate. In their work they assumed the wake to be straight along the flight path. The wings on high-speed ground vehicles, such as racing cars, are another example of lifting surfaces in unsteady ground effect. Normally the wing used in racing cars has negative incidence and an oscillatory heaving motion when the roadway is not perfectly smooth. Katz[11] investigated the performance of automotive lifting surfaces in close proximity to the ground. He considered a rectangular, uncambered wing and investigated the aerodynamic load on a wing oscillating in heave in and out of ground effect. He also investigated the effect of AR. Ando et al.[12] used lifting-surface techniques to analyze a thin two-dimensional airfoil flying over a wavy-wall surface in an incompressible and inviscid flow. The idea of extracting energy from ocean waves for propulsion was investigated by Wu[13] and Grue et al.[14] They found that a hydrofoil moving in incoming waves can extract a relatively large amount of energy. In the present work, we investigate the effect of the waves on a three-dimensional cambered wing flying in air near the surface.

The analysis of a wing in oscillation out of ground effect is valuable also. Not only does it have direct applications such as in aircraft maneuvers, but it also can be used to evaluate the ground effect by comparing the results with those for the wing oscillating near the ground.

The behavior of wakes was studied for an airfoil in oscillation out of ground effect by Katz and Weihs,[15] and more recently by Mook and Dong.[16] In this article, we study the behavior of the wake and the effect of the reduced frequency for a three-dimensional lifting-surface. The loads on a wing oscillating in heave are influenced by the motion of the wing itself, the wake behind the wing, and the distance between the wing and the ground.

II. Aerodynamic Model

We consider an arbitrary curved lifting surface flying at a constant horizontal velocity relative to an inertial reference, over a wavy surface. We limit consideration to the case in which 1) the wavelength of the surface is much greater than the chord of the wing and the height of the wing above surface and 2) the slope of the surface is much less than unity. When this situation is viewed on the scale of the wing, the wavy surface appears to be a plane heaving up and down; thus, the present model simulates a wing flying over swells in the sea. The swells are two dimensional with their troughs and ridges running parallel to the span of the wing.

The situation is represented in Fig. 1: (X, Y, and Z) are the inertial coordinates and (x, y, and z) are the body-fixed coordinates. The body-fixed reference frame translates horizontally to the left at constant velocity: $-V_\infty \boldsymbol{i}$. The time-dependent distance between A, the origin of the moving frame, and surface is given by $h(t)$. Both V_∞ and h are prescribed. The coordinates

Received June 22, 1995; revision received April 19, 1996; accepted for publication May 1, 1996.

*Visiting Assistant Professor, Department of Engineering Science and Mechanics. Member AIAA.
†N. Waldo Harrison Professor, Department of Engineering Science and Mechanics. Associate Fellow AIAA.

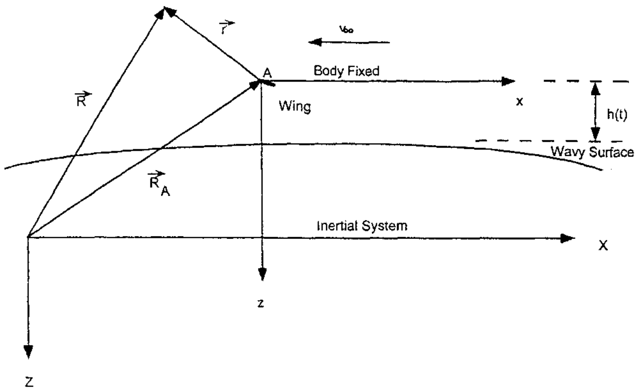

Fig. 1 Description of the coordinate systems over a wavy surface.

of a given point in space in the two systems are related as follows:

$$\boldsymbol{R} = \boldsymbol{R}_A + \boldsymbol{r} \tag{1}$$

where $\boldsymbol{R}$ is the position vector of the point in the inertial system and $\boldsymbol{r}$ is the position vector in the body-fixed system; $\boldsymbol{R}_A$ is the position of the origin of the body-fixed system and is a prescribed function of time. We consider the flow to be incompressible and irrotational everywhere except on the lifting surface and in its wake. In the inertial frame, the flowfield can be described in terms of the velocity potential $\Phi(\boldsymbol{R}, t)$, which satisfies the following:

$$\nabla^2\Phi = 0 \quad \text{in the flowfield} \tag{2}$$

$$(\nabla\Phi + V_\infty \boldsymbol{i})\cdot\boldsymbol{n} = 0 \quad \text{on the surface of the wing} \tag{3}$$

$$\frac{\partial\Phi}{\partial Z} = \dot{h} \quad \text{on the wavy surface} \tag{4}$$

$$\nabla\Phi \to \text{the velocity induced by the wavy surface as } |\boldsymbol{r}| \to \infty \tag{5}$$

where $\boldsymbol{n}$ is a vector normal to the surface of the wing.

Equation (3) is the no-penetration condition on the wing: the normal component of the velocity of a fluid particle in contact with the surface of the wing, relative to the moving surface of the wing, must vanish. Equation (4) is a similar statement for the wavy surface; the overdot denotes the derivative with respect to time, and ∇ is the gradient operator.

It is possible to pose the problem in a more convenient form in terms of another velocity potential ϕ defined as follows:

$$\Phi(\boldsymbol{R}, t) = \phi(\boldsymbol{r}, t) + \dot{h}(t)z \tag{6}$$

The spatial derivatives of Φ are taken with respect to $\boldsymbol{R}$ [i.e., $(X, Y,$ and $Z)$], and those of ϕ are taken with respect to $\boldsymbol{r}$. Because time is constant for these derivatives, the changes in $\boldsymbol{R}$ and $\boldsymbol{r}$ are the same and, hence,

$$\nabla\Phi = \nabla\phi + \dot{h}\boldsymbol{k} \tag{7}$$

$$\nabla^2\Phi = \nabla^2\phi \tag{8}$$

then it follows from Eq. (2) that

$$\nabla^2\phi = 0 \quad \text{in the flowfield} \tag{9}$$

and from Eq. (3) that

$$(\nabla\phi + V_\infty\boldsymbol{i} + \dot{h}\boldsymbol{k})\cdot\boldsymbol{n} = 0 \quad \text{on the surface of the wing} \tag{10}$$

and from Eq. (4) that

$$\frac{\partial\phi}{\partial z} = 0 \quad \text{on the wavy surface} \tag{11}$$

and from Eq. (5) that

$$\nabla\phi \to \boldsymbol{0} \quad \text{as} \quad |\boldsymbol{r}| \to \infty \tag{12}$$

To obtain Eq. (12), we considered the air above the wavy surface to be moving up and down with the surface in the absence of the wing.

It follows from Eqs. (9–12) that ϕ describes the flow over a wing that translates in the vicinity of a fixed surface with the velocity

$$\boldsymbol{V}_{\text{wing}} = -V_\infty\boldsymbol{i} - \dot{h}\boldsymbol{k} \tag{13}$$

through air that is still far from the wing.

The aerodynamic loads on the wing are computed by integrating the pressure over the surface. The pressure is obtained from Bernoulli's equation, which has the following familiar form in terms of Φ:

$$\frac{\partial\Phi}{\partial t} + \frac{\nabla\Phi\cdot\nabla\Phi}{2} + \frac{P}{\rho} = \frac{P_\infty}{\rho} + \frac{\dot{h}^2}{2} \tag{14}$$

The first term is the rate of change of Φ at a given location in the inertial frame of reference; to obtain it, one must vary t while holding $\boldsymbol{R}$ fixed. If $\boldsymbol{R}$ is fixed while t and, hence, $\boldsymbol{R}_A$ vary, then $\boldsymbol{r}$ must also vary. It follows from Eq. (1) that, during a very small time interval Δt

$$\Delta\boldsymbol{r} = -\dot{\boldsymbol{R}}_A\Delta t = (V_\infty\Delta t)\boldsymbol{i} \tag{15}$$

Thus, we convert the time derivatives from ground-fixed coordinates to wing-fixed coordinates as follows:

$$\begin{aligned}\left.\frac{\partial\Phi}{\partial t}\right|_R &= \lim_{\Delta t\to 0}\left[\frac{\Phi(\boldsymbol{R}, t+\Delta t) - \Phi(\boldsymbol{R}, t)}{\Delta t}\right] \\ &= \lim_{\Delta t\to 0}\left[\frac{\phi(\boldsymbol{r} + V_\infty\Delta t\boldsymbol{i}, t+\Delta t) + \dot{h}(t+\Delta t)z - \phi(\boldsymbol{r}, t) - \dot{h}(t)z}{\Delta t}\right] \\ &= \left.\frac{\partial\phi}{\partial t}\right|_r + V_\infty\frac{\partial\phi}{\partial x} + \ddot{h}z\end{aligned} \tag{16}$$

In Eq. (16), the first term is the derivative at a fixed position in the moving reference frame. When Eqs. (7) and (16) are substituted into Eq. (14), the result is

$$\frac{P - P_\infty}{1/2\rho} = -2\left(\frac{\partial\phi}{\partial t} + V_\infty\frac{\partial\phi}{\partial x} + \dot{h}\frac{\partial\phi}{\partial z} + \frac{\nabla\phi\cdot\nabla\phi}{2}\right) - 2\ddot{h}z \tag{17}$$

Equation (17) can be written in terms of nondimensional quantities (denoted by asterisks) as follows:

$$\frac{P - P_\infty}{1/2\rho V_\infty^2} = -2\left(\frac{\partial\phi^*}{\partial t^*} + \frac{\partial\phi^*}{\partial x^*} + \dot{h}^*\frac{\partial\phi^*}{\partial z^*} + \frac{\nabla\phi^*\cdot\nabla\phi^*}{2}\right) - 2\ddot{h}^*z^* \tag{18}$$

The last term makes no contribution to the total aerodynamic loads on the lifting surface. Equations (9–12) are solved by the general unsteady vortex lattice method; an image is used to satisfy Eq. (11).[8] After ϕ is found, Eq. (17) is used to find the pressures; the pressure times a unit normal vector and its moment are integrated over the lifting surface to find the total loads.

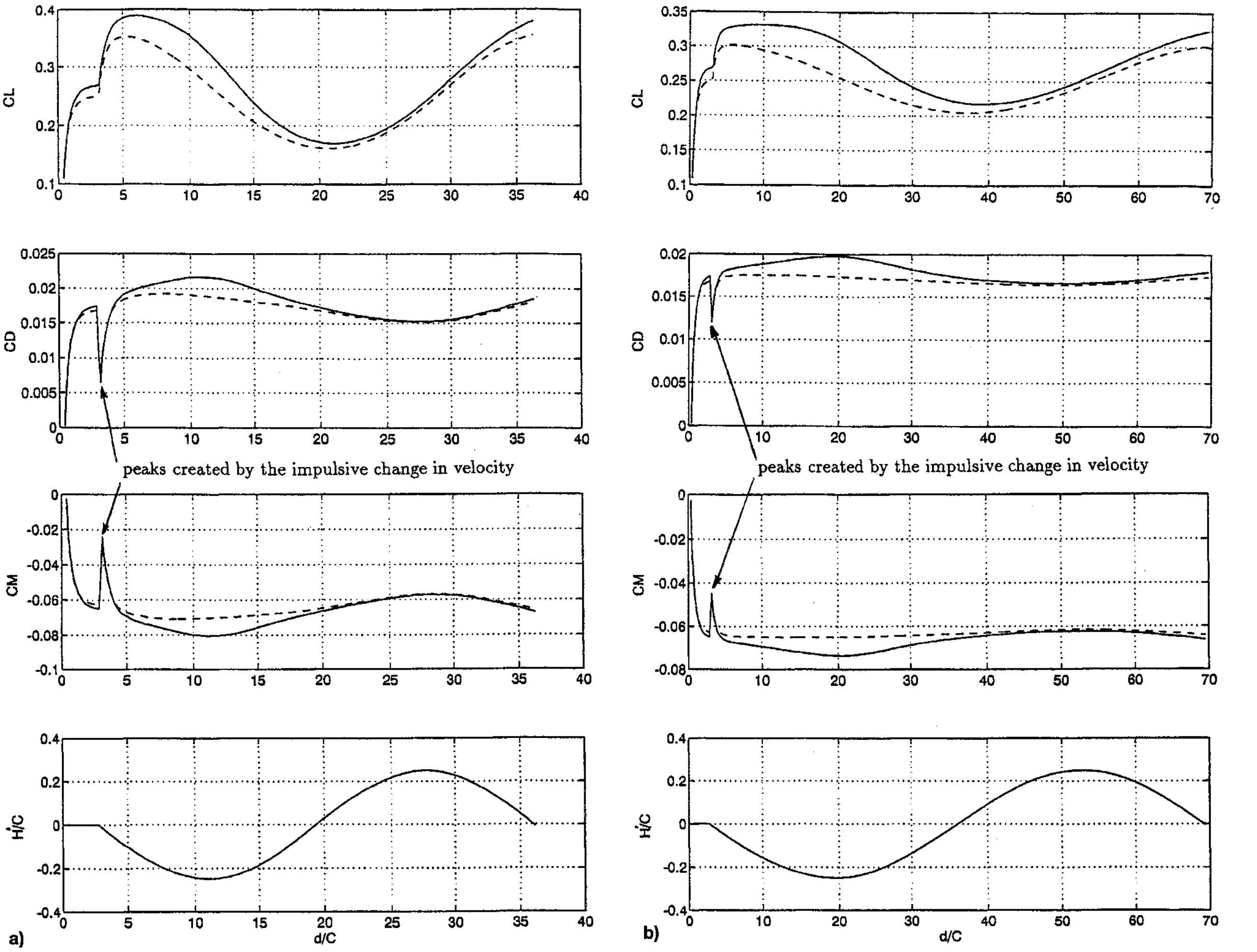

Fig. 2 Lift, drag, moment, and vertical position of the wing with respect to the mean height above the ground as functions of the distance traveled d in terms of chords C. The moment is taken about the quarter chord from the leading edge. —, in ground effect and --, out of ground effect. k = a) $\pi/16$ and b) $\pi/64$.

With the general unsteady vortex–lattice method the lifting surface and the wake are modeled by lattices of discrete vortex filaments. At any instant the circulations around the vortex segments along the edges of a given element are equal; these loop circulations for the lifting surface change with time in an unsteady flow. The position of the vortex lattice representing the body is known. However, the vortex lattice representing the wake deforms freely, always assuming the force-free position.

The time-dependent circulations around the vortex filaments in the bound sheet are determined at each time step by imposing the no-penetration condition at one point in each element (the so-called control point). This no-penetration condition has the form:

$$\sum_{j=1}^{N} A_{ij} G_j = (\boldsymbol{V}_s - \boldsymbol{V}_w) \cdot \boldsymbol{n}_i \tag{19}$$

for $i = 1, 2, \ldots, N$. The variable N is the total number of elements representing the body, and the A_{ij} represents the normal component of the velocity at the control point of the ith element generated by unit circulation around the jth element, and G_j is the unknown circulation around the vortex segments along the edges of the jth element. The vectors $\boldsymbol{V}_s$ and $\boldsymbol{V}_w$ are the velocity of the lifting surface and the velocity induced by the wake at the ith control point, and $\boldsymbol{n}_i$ is the unit vector perpendicular to the elemental area at the control point.

The difference in the pressures on the upper and lower surfaces along the edges where the free and bound vortex sheets are joined is forced to vanish by shedding the segments along these edges into the flowfield. As one segment is shed, another forms. The segments in the wake convect with the flow at the local particle velocity and, hence, occupy the force-free position. Because the vorticity in the wake now was shed from the wing (i.e., determined) earlier, the wake serves as the historian of the flow. When a segment in the wake reaches a point far downstream, it is neglected.

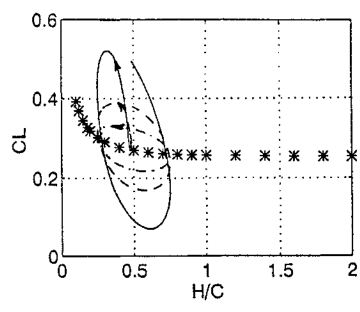

Fig. 3 Comparison of the unsteady lift with the steady-state result. The angle of attack is 3 deg and the mean height is 0.5C. —, $k = \pi/16$; --, $k = \pi/32$; - · -, $k = \pi/64$, and *, steady-state result.

A rectangular cambered wing of unit AR (small ARs are desirable for wingships) oscillating in heave at various mean heights above a plane surface is considered in the present analysis. The time-dependent height of the wing above the ground h is given by $h = H - A \sin \theta$, where A is the amplitude of the oscillation, $\theta = 2\pi t/T = \omega t$, T is the period of the heaving motion, ω is the angular velocity, and t is time. $H' = H - h$ is the vertical position of the wing with respect to the mean height above the ground. The relationship between ω and k is given by $k = \omega C/2V_\infty$, where C is the chord length, V_∞ is the freestream velocity, and k is the reduced frequency.

III. Results

In earlier work,[2,3,7,15] the accuracy of the present model was well established for various two- and three-dimensional steady flows and a few two-dimensional unsteady flows. To further establish confidence in the present method as a model for an oscillating wing, we used it to calculate the loads on a wing with a NACA 0012 profile and an AR of 30 oscillating sinusoidally in pitch about the quarter chord. The numerical results were then compared with the observations of McCroskey et al.[17] The present solution agrees well with the experimental data.

For surface-effect aircraft small ARs are desirable. Because the wingtip vortex systems influence the flow over a significant percentage of the whole wing, small ARs often present difficult problems for classical lifting-surface approximations, but this is not true for the general vortex–lattice method. A rectangular cambered wing of unit AR is used for the remaining examples. The nominal angle of attack for the stationary wing is 3 deg. The amplitude of oscillation is 0.25 chord, C_M is the coefficient of moment about the quarter chord, and C_L is the coefficient of lift.

In Fig. 2, the aerodynamic loads and the vertical position of the wing are shown as functions of the distance traveled for a wing in an oscillatory heaving motion. The mean height of the trailing edge of the wing in ground effect is 0.5 chord. These results were obtained by first fixing the wing at 3-deg angle of attack until a steady state developed and then having it oscillate in heave at an amplitude of 0.25 chord.

The aerodynamic loads are plotted as functions of the distance traveled for $k = \pi/16$ and $\pi/64$, respectively. The differences between the loads in ground effect (solid lines) and those out of ground effect (broken lines) are evident. In both cases and for both frequencies, the peak lift occurs before the peak induced drag and the minimum pitch moment. The symmetry about zero loads is destroyed by the mean angle of attack and the ground.

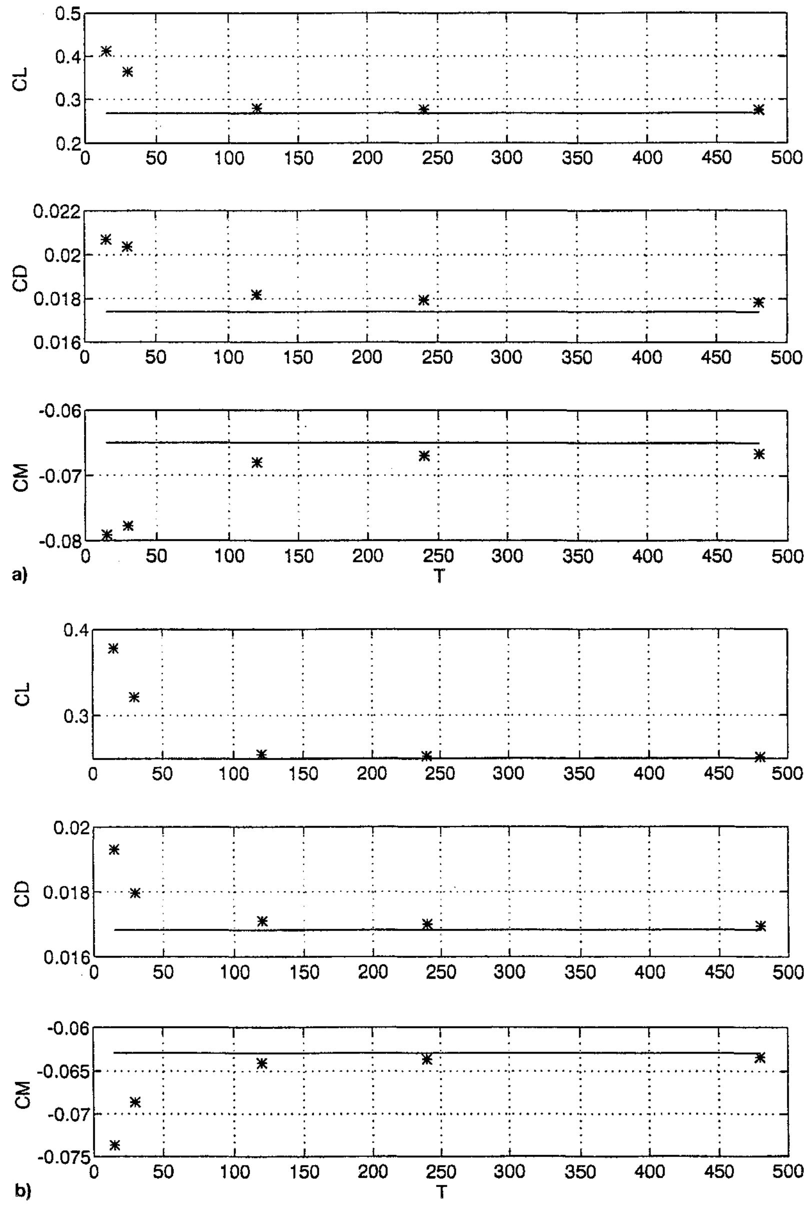

Fig. 4 Comparison of mean values of lift, drag, and moment coefficients for different periods of oscillation with the steady-state result. The mean angle of attack is 3 deg and h = 0.5 chord. —, steady-state ($T = \infty$); and *, mean value during the heaving oscillation. a) In and b) out of ground effect.

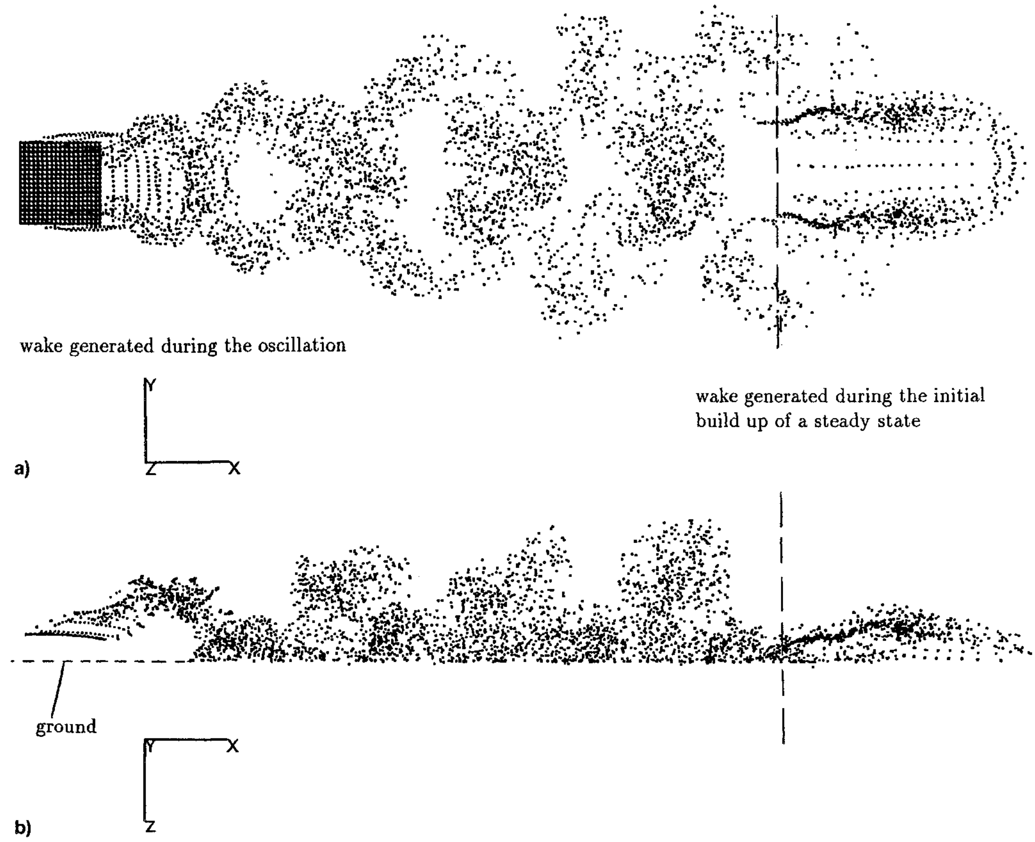

Fig. 5 Computed wakes for the wing in ground effect where $k = \pi/4$, amplitude = 0.25 chord. The dots represent the location of vorticity in the wake of the wing. The portion of the wake generated during the initial startup can be seen at the far right: a) top and b) side view.

As the frequency is decreased, the peaks tend to flatten, last longer, and be smaller. This behavior is more pronounced in ground effect than out. In ground effect, the wing tends to carry the high loads longer.

In Fig. 3 the unsteady aerodynamic lift coefficient is compared with the steady-state result. The wing is in ground effect and the values of reduced frequencies are $\pi/16$, $\pi/38$, and $\pi/64$. It is evident from the figure that as the frequency is decreased, the peak lift coefficients get smaller and closer to the steady-state results. The oscillation tends to dominate the aerodynamic load as the frequency is increased. During a cycle the increase in lift is greater than the decrease, making the mean lift somewhat greater than the value for steady flow.

In Fig. 4a the mean aerodynamic loads for an oscillating wing are compared with those for a wing in steady flow. The wing is in ground effect. The mean aerodynamic load over one cycle is higher than the load in the steady flow at the mean height. The mean aerodynamic load approaches the load in steady flow as the reduced frequency decreases. In Fig. 4b the mean value of the aerodynamic load on an oscillating wing is compared with the load on the wing in steady flow out of ground effect.

Comparing the two sets of results, one finds that the mean loads on the wing in ground effect are higher than those on the wing out of ground effect. The trends, however, are quite similar: the mean lift and induced drag increase with frequency and the moment decreases. Of course, trying to augment the lift by oscillating a wing is not practical, although doing so could raise the mean lift. The present results suggest that the same effect is produced by flying low over a wavy surface, and hence, the waves may actually boost the efficiency of a wingship.

In Fig. 5, the computed wake of the oscillating wing is shown. The dots locate the ends of the discrete vortex segments that represent the wakes. The computations were made by first giving the wing an impulsive start from rest, then having it move forward at constant velocity and angle of attack until the steady state develops, and finally making it oscillate with a simple harmonic motion in heave. The portion of the wake generated during the initial development of the steady state is clearly visible in the figures. The amplitude of the heaving motion is 0.25 chord, the nominal angle of attack is 3 deg, and the mean height is 0.5 chord.

In Fig. 5, the reduced frequency of the oscillation is a rather high $\pi/4$. In this figure, the top and side views are shown and the wing is flying near the ground. In the figure one sees that the ground clearly restricts the vertical extent of the wakes and increases the horizontal extent. Spreading the wake horizontally generally has the beneficial effect of making the wing appear to have a larger AR than it actually does.

In this figure the wing is approaching the low point of its trajectory. Near the low points of the trajectory, the wing develops more lift and hence sheds more vorticity than the wing out of ground effect, and the corresponding portions of the two wakes have very different forms. The wake near the ground spreads horizontally in both the crossflow and streamwise directions more than the other wake. In contrast, near the high points of the trajectories, both wings shed about the same vorticity and the corresponding portions of their wakes have similar forms. The different positions of the wakes mean that their influence on the flowfields around the tail assemblies in and out of ground effect will be somewhat different. The use of low-AR wings makes the difference more noticeable.

IV. Concluding Remarks

Recent interest in transoceanic ground effect airplanes raises the question of what effect the waves and large swells would have on the performance. Would they enhance or degrade the benefits that can be derived from operating near the surface? As a first attempt to simulate a wing flying over a wavy surface, we have considered small-AR, slightly cambered wings flying over long-wavelength ocean swells. The mean aerodynamic loads on a wing oscillating in heave at a nominal angle of attack are higher than the corresponding loads on a wing in steady flight at the same angle of attack. This result is true for wings operating both near and far from the ground. The increases are about the same in both cases. Moreover, they grow as the frequency increases, even reaching the point at a rather high frequency where the effects of the oscillation completely dominate those of the ground. Of course, oscillating a wing to augment its aerodynamic performance is not practical, but flying near a wavy surface may well be, and the effects appear to be similar. Thus, we conclude from this preliminary study that flying over a wavy surface probably would enhance the efficiency of a ground-effect craft and, hence, be rather beneficial.

Acknowledgment

This work was supported by the U.S. Air Force Office of Scientific Research under Grant AFOSR-90-0032.

References

[1]Dane, A., ''Wingships,'' *Popular Mechanics*, May 1992, pp. 35–38.

[2]Belotserkovskii, S. M., ''Study of the Unsteady Aerodynamics of Lifting Surfaces Using the Computer,'' *Annual Review of Fluid Mechanics*, Vol. 9, 1977, pp. 469–494.

[3]Mook, D. T., and Maddox, S. A., ''Extension of a Vortex-Lattice Method to Include the Effects of Leading Edge Separation,'' *Journal of Aircraft*, Vol. 11, No. 2, 1974, pp. 127, 128.

[4]Konstadinopoulos, P., Thrasher, D. F., Mook, D. T., Nayfeh, A. H., and Watson, L., ''A Vortex-Lattice Method for General Unsteady Aerodynamics,'' *Journal of Aircraft*, Vol. 22, No. 1, 1985, pp. 43–49.

[5]Steven, V. C., ''The Ground Effect of a Power-Lift STOL Aircraft During Landing Approach,'' *Proceedings of the 1985 NASA Ground Effect Workshop*, NASA CP-2462, 1985.

[6]Licher, R. M., ''Increases in Lift for Two and Three-Dimensional Wings Near the Ground,'' Douglas Aircraft, Santa Monica Div., Rept. SM-22615, Oct. 1956.

[7]Tuck, E. O., ''Hydrodynamic Problems of Ships in Restricted Waters,'' *Annual Review of Fluid Mechanics*, Vol. 10, 1978, pp. 33–44.

[8]Nuhait, A. O., and Mook, D. T., ''Numerical Simulation of Wings in Steady and Unsteady Ground Effects,'' *Journal of Aircraft*, Vol. 26, No. 12, 1989, pp. 1081–1089.

[9]Chang, R. C., ''An Experimental Investigation of Dynamic Ground Effect,'' Ph.D. Dissertation, Dept. of Aerospace Engineering, Univ. of Kansas, Lawrence, KS, 1985.

[10]Chen, Y. S., and Schweikhard, W. G., ''Dynamic Ground Effects on a Two-Dimensional Flat Plate,'' *Journal of Aircraft*, Vol. 22, No. 7, 1985, pp. 638–640.

[11]Katz, J., ''Calculation of the Aerodynamic Forces on Automotive Lifting Surfaces,'' *Journal of Fluids Engineering*, Vol. 107, Dec. 1985, pp. 438–443.

[12]Ando, S., Sakai, T., and Nitta, K., ''Analysis of Motion of Airfoil Flying over Wavy-Wall Surface,'' *Japan Society of Aerospace Science*, Vol. 35, No. 107, 1992, pp. 27–38.

[13]Wu, T. Y., ''Extraction of Flow Energy by a Wing Oscillating in Waves,'' *Journal of Ship Research*, 1972, pp. 66–78.

[14]Grue, J., Mo, A., and Palm, E., ''Propulsion of a Foil in Water Waves,'' *Journal of Fluid Mechanics*, Vol. 186, 1988, pp. 393–417.

[15]Katz, J., and Weihs, D., ''Behavior of Vortex Wakes from Oscillating Airfoils,'' *Journal of Aircraft*, Vol. 15, No. 12, 1978, pp. 861–863.

[16]Mook, D. T., and Dong, B., ''Perspective: Numerical Simulations of Wakes and Blade-Vortex Interaction,'' *Journal of Fluids Engineering*, Vol. 116, March 1994, pp. 5–21.

[17]McCroskey, W. J., McAlister, K. W., Carr, L. W., Pucci, S. L., Lambert, O., and Indergrand, R. F., ''Dynamic Stall on Advanced Airfoil Sections,'' *Journal of the American Helicopter Society*, July 1981, pp. 40–50.